The endocranium of the theropod dinosaur *Ceratosaurus* studied with computed tomography

R. KENT SANDERS and DAVID K. SMITH

Sanders, R.K. and Smith, D.K. 2005. The endocranium of the theropod dinosaur *Ceratosaurus* studied with computed tomography. *Acta Palaeontologica Polonica* 50 (3): 601–616.

A well preserved specimen of the theropod *Ceratosaurus* from the Upper Jurassic Morrison Formation of western Colorado was recently described and given the name *C. magnicornis*. The systematics of the genus is outside the scope of the present study but, as a generally accepted basal tetanuran, the braincase was CT scanned to provide a description of the endocranium, inner ear, pneumatic, and venous sinus systems in a primitive member of this clade. Five major subregions of the theropod endocranium are distinguished for the purpose of simplifying cranial computed tomographic interpretation and to provide a systematic means of comparison to other endocrania. The skull morphology of *Ceratosaurus* influences the overall braincase morphology and the number and distribution of the major foramina. The low pontine angle and relatively unflexed braincase is considered a more primitive character. The orientation of the horizontal semicircular canal confirms a rather horizontal and unerect posture of the head and neck. As in birds, the narrower skull morphology of *Ceratosaurus* is associated with fewer cranial nerve foramina. Additionally, the maxillary dominated dentigerous upper jaw of *Ceratosaurus* is felt to share with the alligator a large rostrally directed maxillary division of the trigeminal nerve and a small ophthalmic branch. The upper bill of birds, being dominated by the premaxillary and lacking teeth, is innervated predominantly by the ophthalmic division of the trigeminal nerve. For this reason, avian-based cranial nerve reconstructions are felt to be inappropriate for basal theropods. *Ceratosaurus* skull pneumatization and possible evidence of olfactory conchal structures is on the other hand very avian in character. Based on computed tomography, *Ceratosaurus* is determined to have possessed a typical basal theropod endocranium and bipedal vestibular system similar to *Allosaurus*.

Key words: Theropoda, *Ceratosaurus*, endocranium, paleoneurology, cranial pneumatic systems, computed tomography, virtual rendering.

R. Kent Sanders [kent.sanders@hsc.utah.edu], Assistant Professor of Radiology University of Utah HSC, 50 North Medical Drive, 1A71, Salt Lake City, Utah 84132, U.S.A.;
David K. Smith [dks32@email.byu.edu], Earth Science Museum, Brigham Young University, Provo, Utah 84602, U.S.A.

Introduction

A large, well-preserved braincase of *Ceratosaurus* (MWC 1, Fig.1) from the Brushy Basin Member of the Upper Jurassic Morrison Formation near Fruita, Colorado was recently described by Madsen and Welles (2000). It was associated with much of the rest of the skeleton and given the name *Ceratosaurus magnicornis*. Although this designation has been questioned (Rauhut 2003), that topic lies outside the realm of the present study. Unlike the braincase in the type specimen of *Ceratosaurus nasicornis* from Cañon City described by Gilmore (1920), the Fruita specimen is minimally distorted.

Ceratosaurus is currently regarded as a primitive tetanuran theropod (Rauhut 2003). As such, we CT-scanned the Fruita specimen in order to describe the endocranial cavity, pneumatic system, and ear region in an attempt to establish the ancestral condition in this clade. A generalized endocranial reconstruction based on the type of *Ceratosaurus nasicornis* was published by Marsh (1896), but it is extremely idealized. Several more derived theropod endocrania were recently described in the literature, including *Allosaurus* (Hopson 1979), *Tyrannosaurus* (Brochu 2000), and *Carcharodontosaurus* (Larsson 2001), and these are used for comparison with the present, updated, description of this part of *Ceratosaurus*.

Based on the results for *Ceratosaurus*, we propose a system of analyzing endocranial anatomy of fossil skulls as revealed by computed tomography. These results are used to organize this complicated aspect of cranial anatomy and hopefully facilitate future comparisons. We also address variation in skull foraminal patterns as a function of skull morphology and present selected phylogenetically bracketed (Witmer 1997a) comparative anatomy in extant birds and crocodilians. Finally, we present three-dimensional virtual reconstructions of the various endocranial anatomical systems of MWC-1 as revealed by CT.

Methods and materials

The *Ceratosaurus* braincase was scanned in the short axis, or coronal plane, in three millimeter slice thickness with one millimeter overlap using a GE Lightspeed quad detector. A

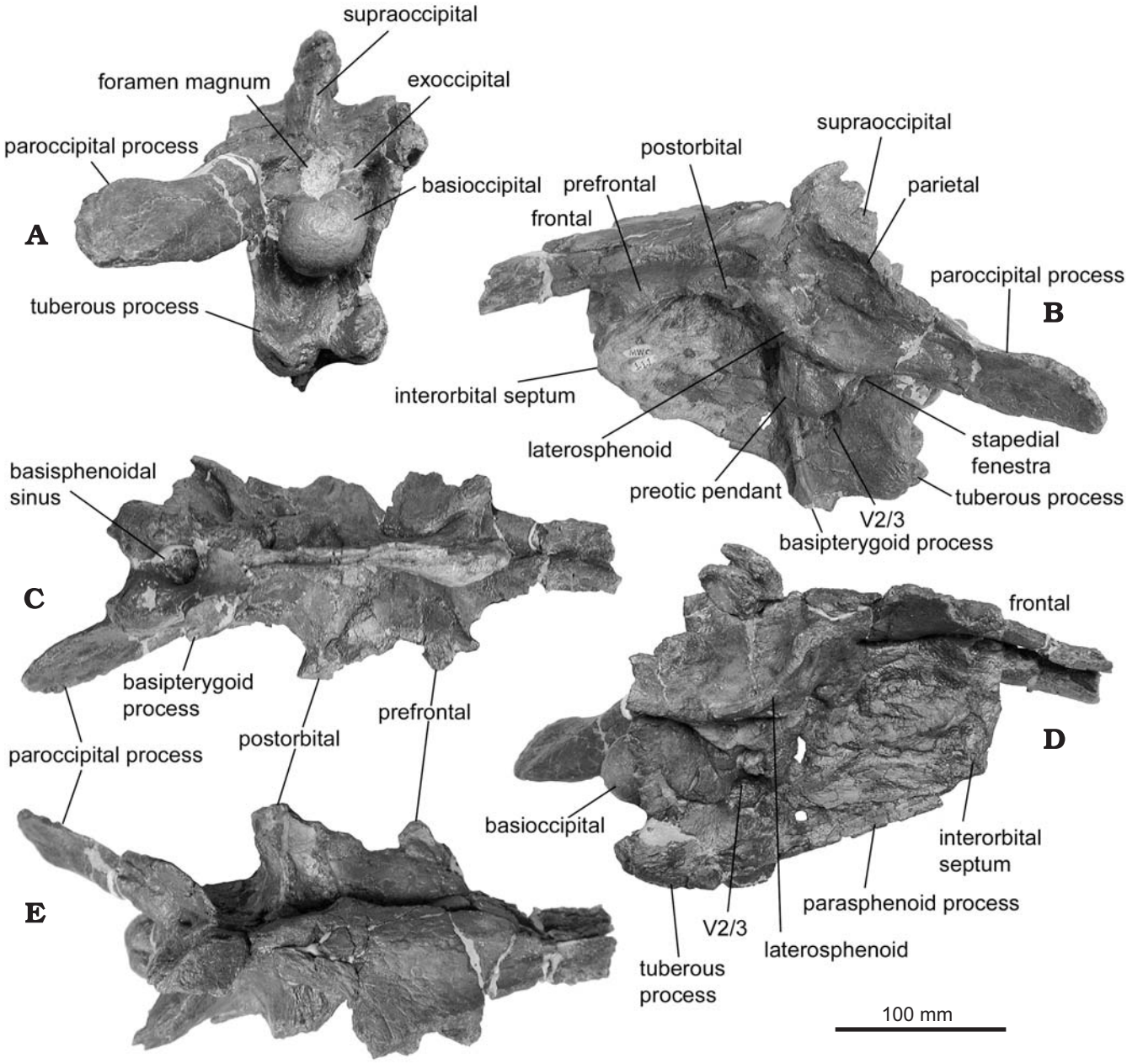

Fig. 1. *Ceratosaurus magnicornis* (MWC 1, Fruita, Colorado, Morrison Formation, Upper Jurassic). Specimen photographs of the braincase in posterior (**A**), left lateral (**B**), ventral (**C**), right lateral (**D**), and dorsal (**E**) views.

soft tissue algorithm was used to reduce the effects of beam hardening artifact. Within the inner ear, oblique planar reconstructions were made of the semicircular canals and associated structures using a GE Advantage Windows Imaging Processing Workstation. The final three-dimensional reconstruction of the endocranium, inner ear, pneumatic cavities, and venous structures was created using Surfdriver, a commercially available, inexpensive, and PC compatible volume rendering program. This reconstruction was then compared with theropod endocranial descriptions in the literature, and extant bird and crocodilian skulls.

Institutional abbreviations.—The described specimen is housed at the Museum of Western Colorado (MWC) in Fruita, Colorado. Comparative specimens include an *Allosaurus* endocast from the University of Utah Vertebrate Paleontology collection (UUVP) in Salt Lake City, Utah. Extant comparative anatomical specimens include an embalmed ostrich head (*Struthio camellus*) from the Louisiana State University School of Veterinary Medicine (LSU-SVM) Comparative Biomedical Sciences department, Baton Rouge, Louisiana, and an embalmed alligator head (*Alligator mississippiensis*) procured from the Rockerfeller Wildlife Refuge in cooperation with the Louisiana Department of Wildlife and Fisheries (LDWF).

Other abbreviations.—CT, computed tomography; MRI, magnetic resonance image.

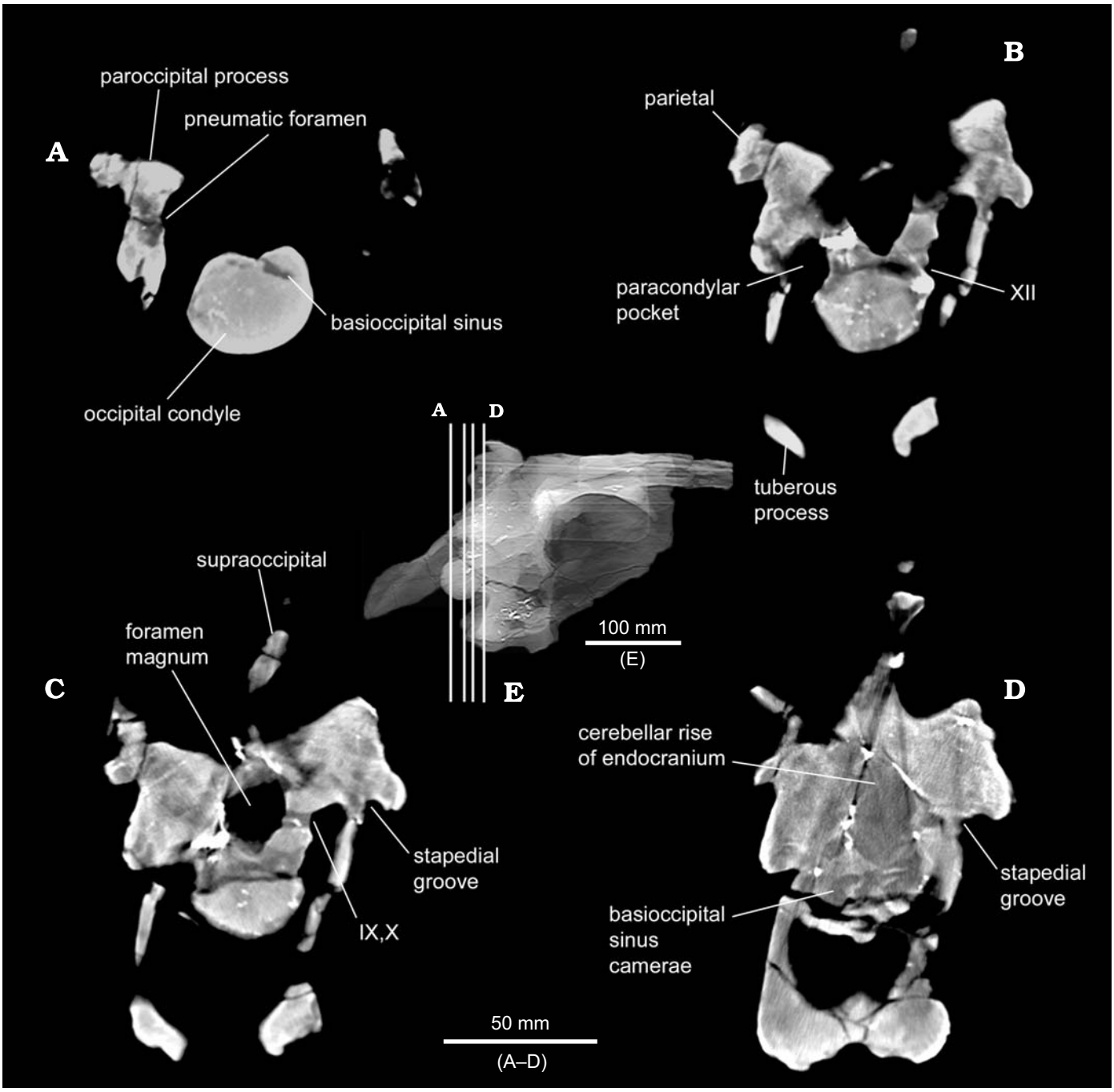

Fig. 2. *Ceratosaurus magnicornis* (MWC 1, Fruita, Colorado, Morrison Formation, Upper Jurassic). **A**–**D**. Computed tomograms of the occipital zone. **E**. Right lateral view of the whole braincase with vertical white lines indicating positions of sections A–D.

Description

The internal anatomy of the endocranium is presented from a caudal to rostral sequence. This arrangement coincides with the sequence of CT image presentation and allows the neural structures to be easily divided into functional anatomic zones that reflect the organization of the brain and numbered cranial nerves. Endocranial skeletal landmarks provide for easy identification of the five anatomic zones and will serve to organize future endocranial anatomic comparison.

Zone 1: Occipital (Fig. 2).—The foramen magnum measures 28.4 mm dorsoventrally and 19.9 mm transversely, resulting in a height to width ratio of 1.4. The occipital condyle measures 40.9 mm dorsoventrally and 34.2 mm transversely, giving a height to width ratio of 1.2. The occipitofrontal angle (Fig. 3A) is obtuse and compares well to *Sinraptor*, (Coria and Currie 2003). However, the brain endocast exhib-

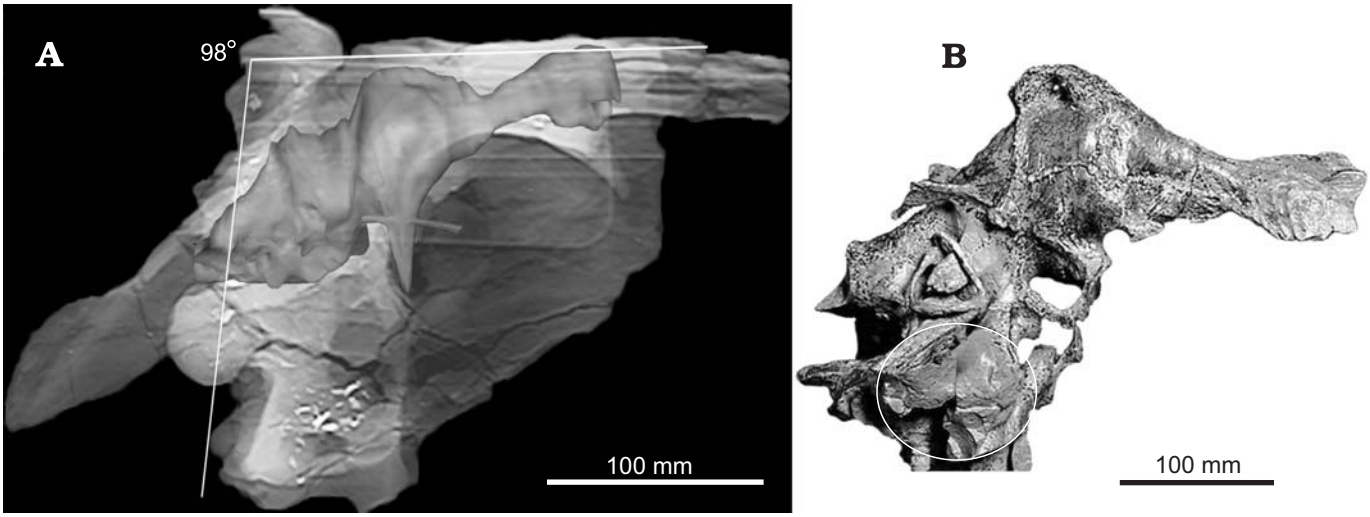

Fig. 3. **A**. *Ceratosaurus magnicornis* (MWC 1, Fruita, Colorado, Morrison Formation, Upper Jurassic), computed tomography image of the whole braincase in right lateral view with superimposed digital endocast (dark outline). The occipitofrontal angle is 98°. **B**. *Allosaurus fragilis* (UUVP 294, Cleveland-Lloyd Quarry, Morrison Formation, Jurassic) endocranial cast (from Rogers 1998). Matrix below the semicircular canals in an oval white outline represents epipharyngeal pneumatic sinuses and is not part of the endocranium. Note that endocast of *Ceratosaurus* is straighter than in *Allosaurus*.

its a less acute pontine angle than in some theropods, such as *Allosaurus*, giving the brain endocast a rather unflexed morphology (Fig. 3). In many theropods, the hypoglossal foramen exits at the dorsolateral base of the occipital condyle near its junction with the foramen magnum but in this specimen of *Ceratosaurus*, there is a transversely oriented crack distorting this region. The combined foramen for the passage of the glossopharyngeal and vagus nerves (IX and X) is an easily recognized, ventrolaterally projecting, foramen that marks the rostral margin of the occipital zone. This is similar to *Allosaurus* (Hopson 1979). The vestibular apparatus is found immediately rostral to this combined foramen.

Zone 2: Otic (Fig. 4).—The vestibulocochlear apparatus, with its associated cranial nerves, is the major structure of the otic region. The prominent stapedial groove is the caudalmost external otic structure. The stapedial groove, along with any associated tympanic recesses, define the skeletal component of the middle ear. It is an elongate fissure leading to the lateral foramen ovale that provides the pathway for the collumella and its stapedial footplate. The groove extends rostrally to a point dorsal to the crista prootica and rostral to the jugular foramen (Madsen and Welles 2000). Its medial rostral apex ends in the lateral margin of the utriculocochlear junction of the inner ear.

In birds, there may be multiple tympanic recesses present in the middle ear (Kuhne and Lewis 1985), while in crocodilians the middle ear contains only a single recess (Wever 1978). The Eustachian, or pharyngotympanic tube, normally communicates form the oropharynx to the middle ear cavity allowing for equilibration of air pressure within the middle ear. In this specimen of *Ceratosaurus*, a distinct eustachian tube was not detected but the apex of the stapedial groove is intimately associated with the roof of the basisphenoidal sinus complex and on the left side, a communication is preserved between the sinus and the stapedial groove rostral to the utricular junction.

The vestibular apparatus is easily recognized on cross-sectional images as a set of uniform holes that, by paging back and forth through the images, can be seen to form interlocking loops in the temporal condensation of the sphenoid (Fig. 4). In MWC 1, the inner ear is best observed on the right side, as metallic inclusions in the left ear obscure this region with beam hardening artifact. The semicircular canals are oriented at right angles to each other with the left and right canal arrays being positioned 90° from each other. The anterior semicircular canals are oriented 45° from the sagittal plane of the skull. If the horizontal canal is oriented parallel to the ground surface, as would be expected in the locomotory and alert postures (De Beer 1947; Dujim 1951; Erichsen 1989), the skull is slightly upturned at the snout with the dorsal surface of the skull being also parallel to the ground surface. The craniocervical posture then would be minimally flexed, indicating a nearly horizontal spine and head orientation.

The vestibulocochlear complex is similar to those of *Allosaurus* and *Carcharodontosaurus* (Rogers 1999; Larsson 2001). The semicircular canals of *Ceratosaurus* are large (Fig. 5), but not as triangular as in *Carcharodontosaurus*. Orthogonal canal arch diameters, as measured from the center of the canals/ampullae, are: anterior (23 by 14 mm), posterior (19.5 by 5 mm), and horizontal (20 by 3.5 mm). The horizontal canal has the shallowest arch configuration while the anterior is the deepest. The anterior semicircular canal arches dorsally above the level of the smaller posterior canal and is more triangular in morphology than the more arcuate posterior and lateral canals. This degree of elongation of the anterior canal reflects is role in stabilizing the head and eyes during bipedal locomotion and is typical of nonavian therapods (Sipla et al. 2004). The junction of the anterior and posterior

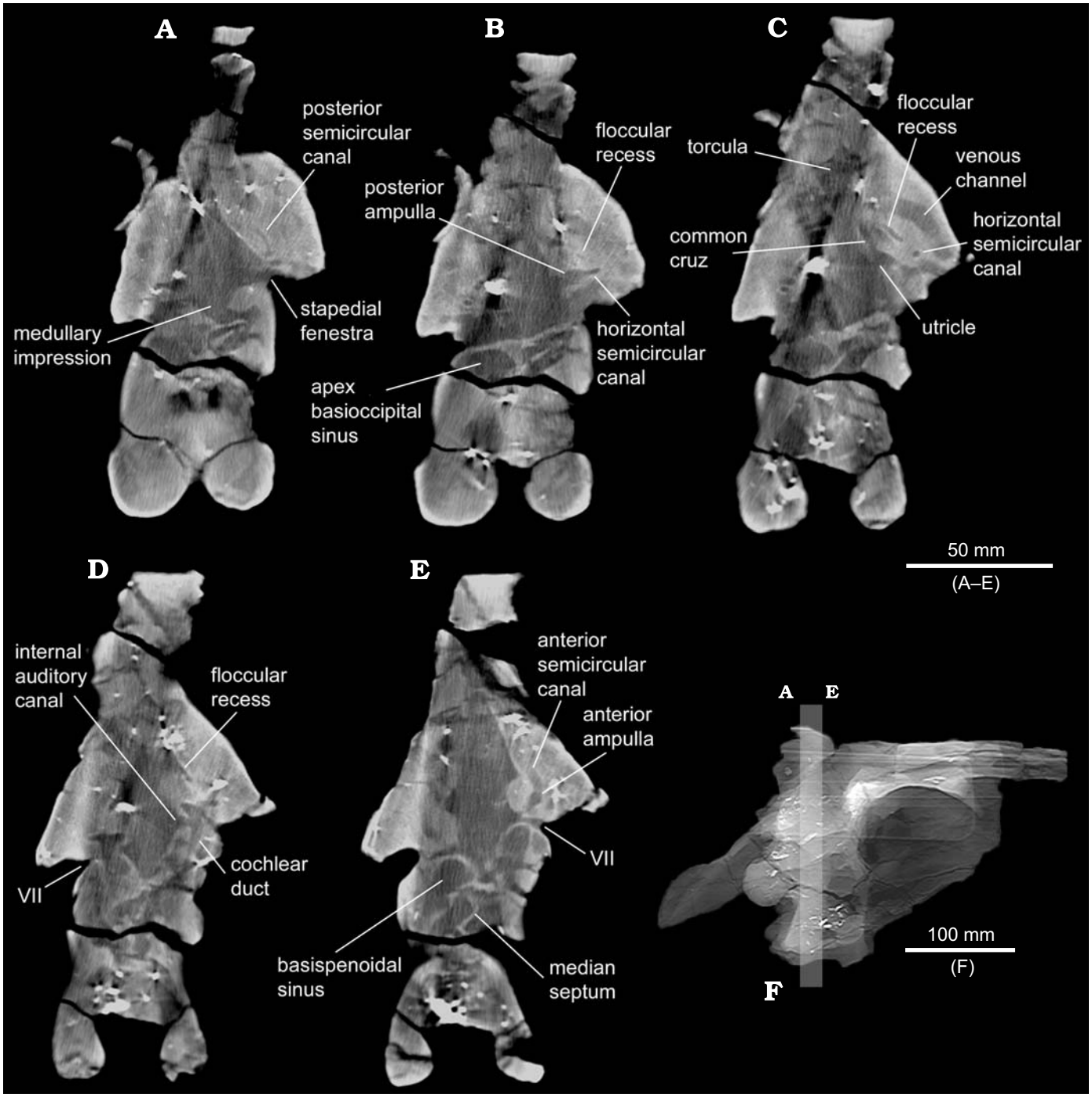

Fig. 4. *Ceratosaurus magnicornis* (MWC 1, Fruita, Colorado, Morrison Formation, Upper Jurassic). **A**–**E**. Computed tomograms of the otic zone. **F**. Right lateral view of the whole braincase with semitransparent slab indicating location of the sections.

canals, at the dorsal margin of the common cruz, is inclined posteriorly. The common cruz extends to meet the medial side of the utricle. The posterior and horizontal canals appear to fuse at the ampulla of the posterior canal. This condition differs from crocodilians in which the posterior horizontal canal arises from the inferior common cruz (Wever 1978). A total of three ampullae are recognized. The anterior fusion of the horizontal canal with the utricle ends in the horizontal canal ampulla immediately caudal to the larger ampulla of the anterior canal. The anterior canal ampulla is the most rostral structure of the vestibulocochlear complex.

The combined utricular and sacular cavity is shaped like a blunt inverted tetrahedron with its elongated apex becoming the cochlear duct (Fig. 5). The cochlear duct projects ventrally from the utricle at a point slightly anterior to the junction of the utricle with the common cruz. From the inferior margin of the oval foramen to its ventral tip, the cochlear duct is about 7 mm long.

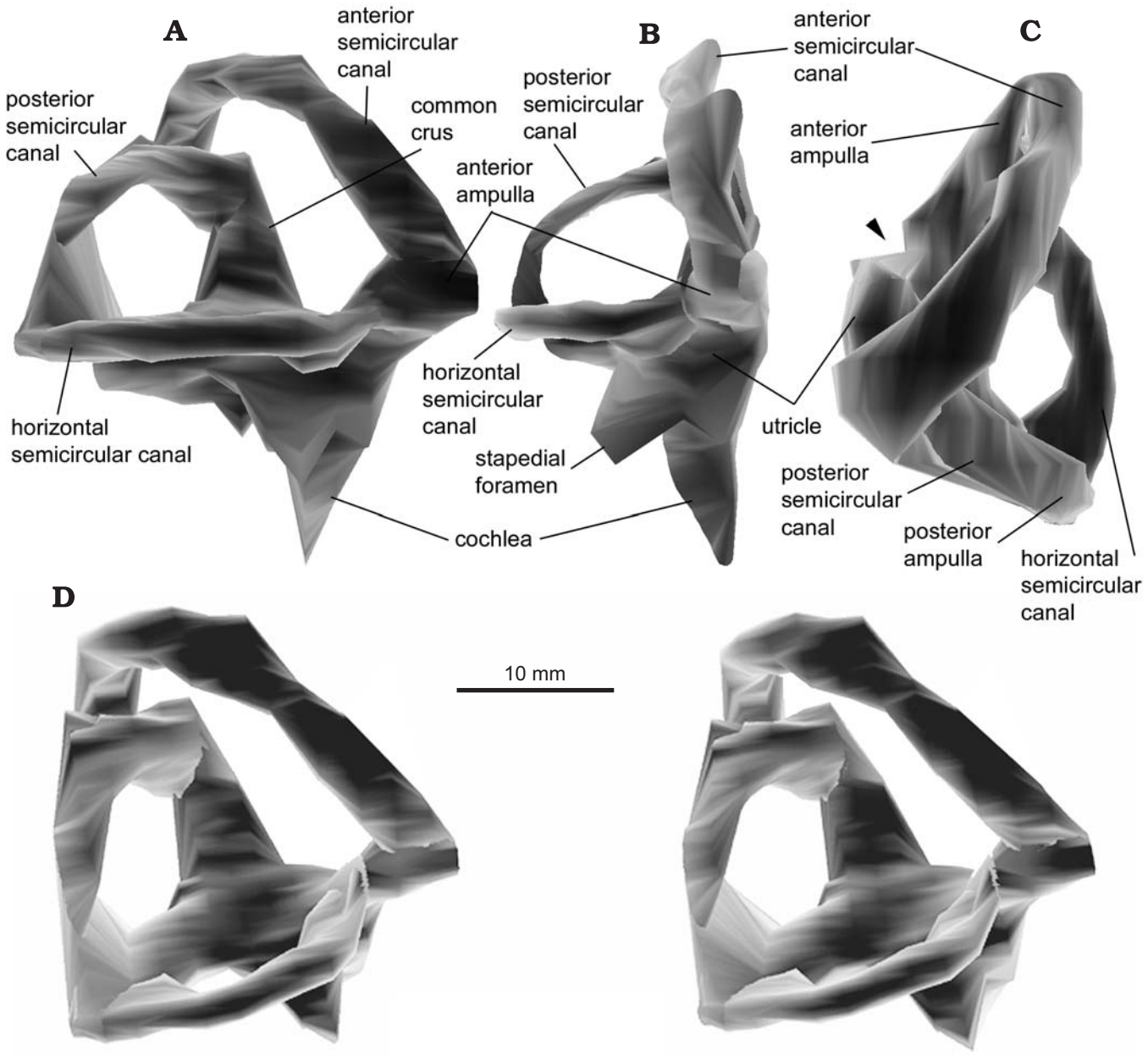

Fig. 5. Three dimensional reconstruction of the inner ear of *Ceratosaurus magnicornis* (MWC 1) in lateral (**A**), anterior (**B**), and dorsal (**C**) views. An arrowhead points to a reconstruction artifact at junction of anterior semicircular canal and utricle. **D**. A stereopair in the dorsolateral view.

There is a small, wedge-shaped flocculus that projects posterolaterally into the center of the semicircular canal array between the anterior canal and common cruz. The internal auditory canal (VIII) is a conical opening between the medial surface of the utricle and endocranium. The rostral margin of the internal auditory canal is closely associated with a smaller, more rostral, parallel canal that terminates rostral to the utricle. The location of this canal, near the apex of the stapedial groove and the oval foramen/stapedial footplate probably accommodated the facial nerve (VII) as it is consistent with the position of this nerve as it extends towards the stapedius muscle or its equivalent. The facial nerve foramen is the most rostral structure of the otic region.

The floor of the endocranial cavity in the otic zone is impressed by the pons at the pontine flexure of the brain. The flexure consists of a rounded depression in the floor of the endocranium that rises from the more ventral medullary level to the more dorsal optic tract level at the roof of the pituitary fossa. The abrupt flattening of the endocranial floor rostral to the depression of the pontine flexure marks the root of the exiting trigeminal trunks that constitute the caudal boundary of the next endocranial zone.

Zone 3: Trigeminal (Fig. 6).—The next rostral cranial foramen is the large and easily recognized trigeminal foramen (CN V). As observed by Witmer (1995), the branches of the

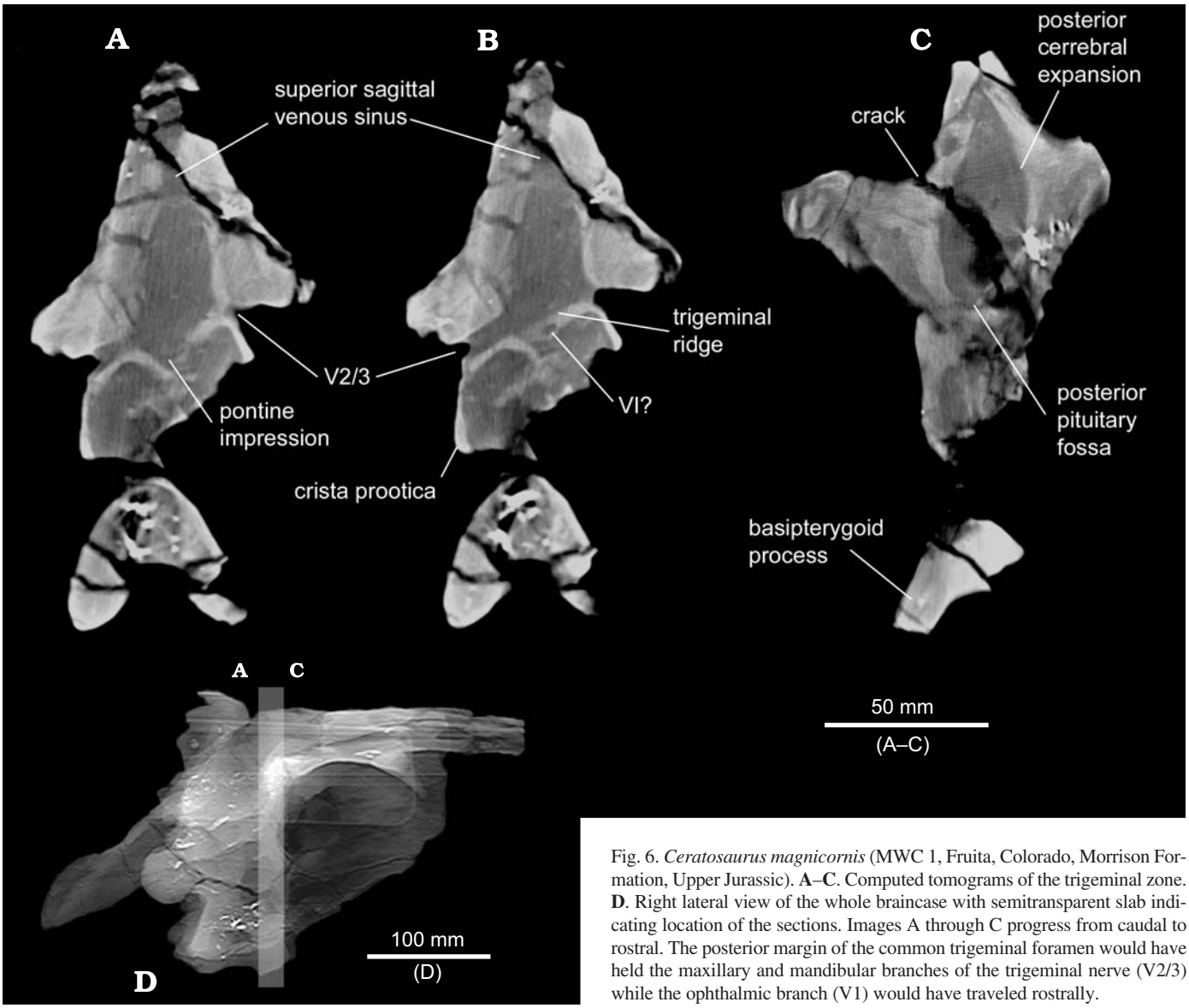

Fig. 6. *Ceratosaurus magnicornis* (MWC 1, Fruita, Colorado, Morrison Formation, Upper Jurassic). **A–C**. Computed tomograms of the trigeminal zone. **D**. Right lateral view of the whole braincase with semitransparent slab indicating location of the sections. Images A through C progress from caudal to rostral. The posterior margin of the common trigeminal foramen would have held the maxillary and mandibular branches of the trigeminal nerve (V2/3) while the ophthalmic branch (V1) would have traveled rostrally.

trigeminal nerve display "highly conserved topographic relationships [that] have long been used as landmarks in [anatomical] studies". The trigeminal ganglion arises from a large nerve trunk that emerges from the base of the brain at the pons. In *Ceratosaurus*, the rounded pontine expansion of the midbrain ends at the trigeminal trunk and the floor of the endocranium flattens abruptly. No trigeminal ganglion impression (Meckel's cave) is observed. The abducens nerve (VI) typically arises from the pons, medial to the trigeminal trunks, at the midline of the brain. As this nerve proceeds rostrally towards the orbit to its extraocular muscle, a ventrally directed foramen should not be expected. However, there is a single midline opening, less than 3 mm in diameter, immediately rostral to the trigeminal trunk in MWC 1. This foramen is only observed on 2 slices. It may represent the abducens nerve, occulomoter nerve, or a combined neurovascular opening. In the alligator, the cranial nerves III, IV, and VI enter the orbit through the orbital fissure (Chiasson 1962), while in the quail these same nerves share the optic nerve foramen with cranial nerve II (Fitzgerald 1969).

In evaluating the effect of skull width on trigeminal nerve foraminal pattern, we examined foraminal patterns in extant bird skulls with variable widths across the basiocciput. It should be noted that brain width may not directly correspond with skull width. Cranial nerves travel a longer and more divergent distance from the brain before encountering the confines of the outer skull in broad skulls, while diverging less in narrow ones. In general, more foraminal openings were observed in wider and more pneumatically inflated skulls. Therefore, narrow skulls typically have fewer foramina that may accommodate multiple cranial nerves, while broad skulls may be characterized by discrete foramina for each cranial nerve. In the narrow skull of *Ceratosaurus*, there are relatively few cranial foramina, suggesting that closely located cranial nerves shared common foramina. For instance, the trigeminal trunk divides into its three branches lateral to the ganglion, but

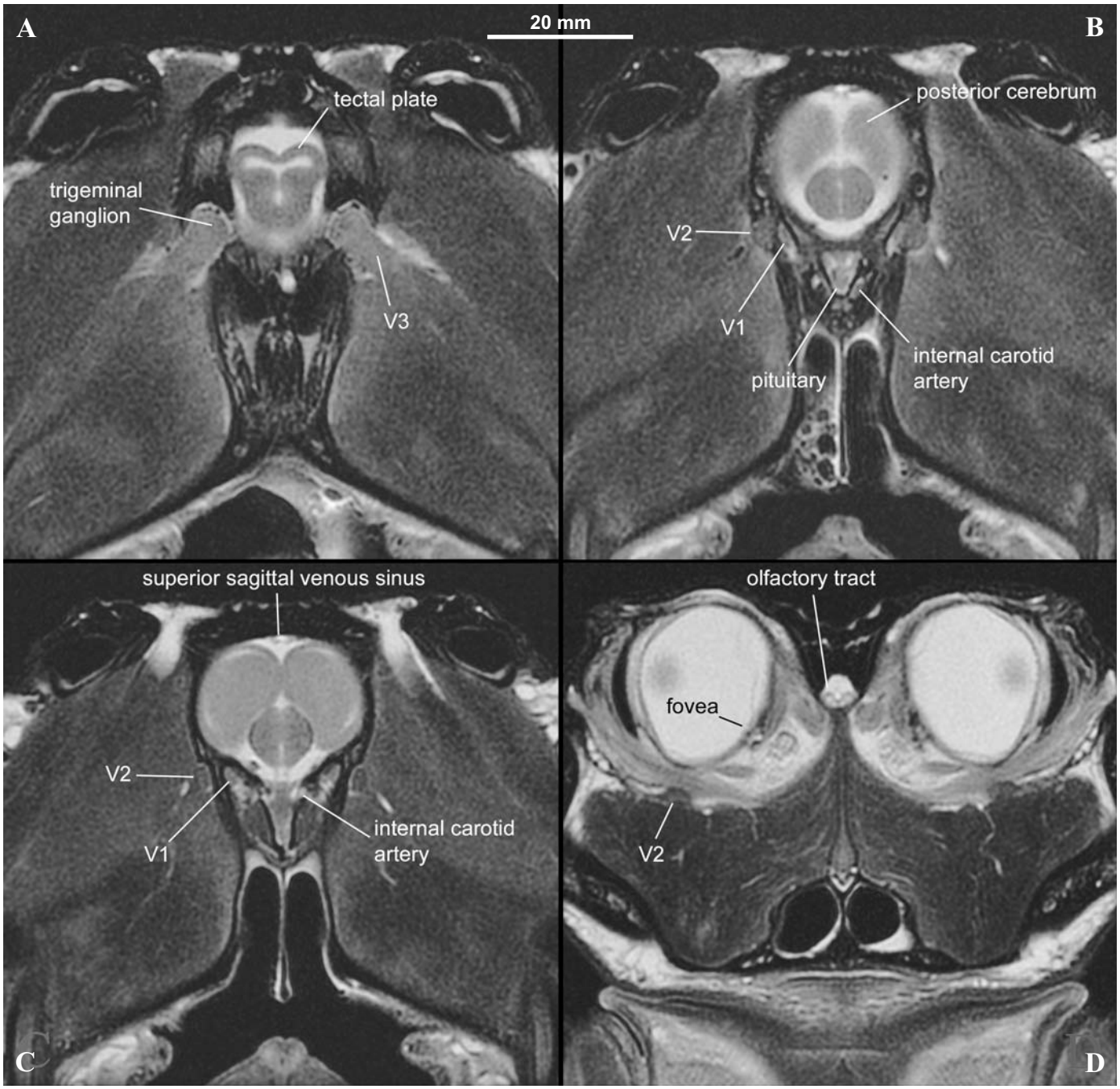

Fig. 7. *Alligator mississippiensis* (LDWF 904625, Recent). Coronal T2 weighted fast spin echo MRI of showing branches of the trigeminal nerve. The images progress from caudal to rostral. **A**. The caudalmost slice shows the trigeminal ganglion and the large mandibular branch (V3) entering the jaw muscle complex. **B**. Proximal maxillary branch (V2) exiting skull at apex of pterygoid space while the proximal ophthalmic branch (V1) travels towards the orbit inside the skull. **C**. V1 in the roof of the cavernous sinus, V2 outside the skull and prior to entering the posterior orbital floor next to the recurrent loop of the internal carotid artery. This section of the carotid artery is proximal to the anterior and posterior encephalic arteries (Burda 1969). **D**. V2 traversing the floor of the orbit before entering the snout. All sections are in the same scale.

there is only one very large trigeminal opening, so the trifurcation likely occurred outside of the basicranium

A large proportional difference in trigeminal nerve branch size was observed in birds. The ophthalmic branch is the smallest while the maxillary/mandibular divisions show the greatest expansion in diameter. The largest ophthalmic divisions were found in long billed birds such as the pelican (*Pelicanus erythrorhynchos*), and in filter feeding ducks like the shoveler (*Anas clypeata)*. Each of these groups of birds have numerous and extensive neurovascular structures providing support for the keratin covering and sensation throughout the upper bills. The upper jaw in birds is dominated by the premaxilla, which is mostly supplied by the ophthalmic branch of the trigeminal. Dentulate dinosaurs had the

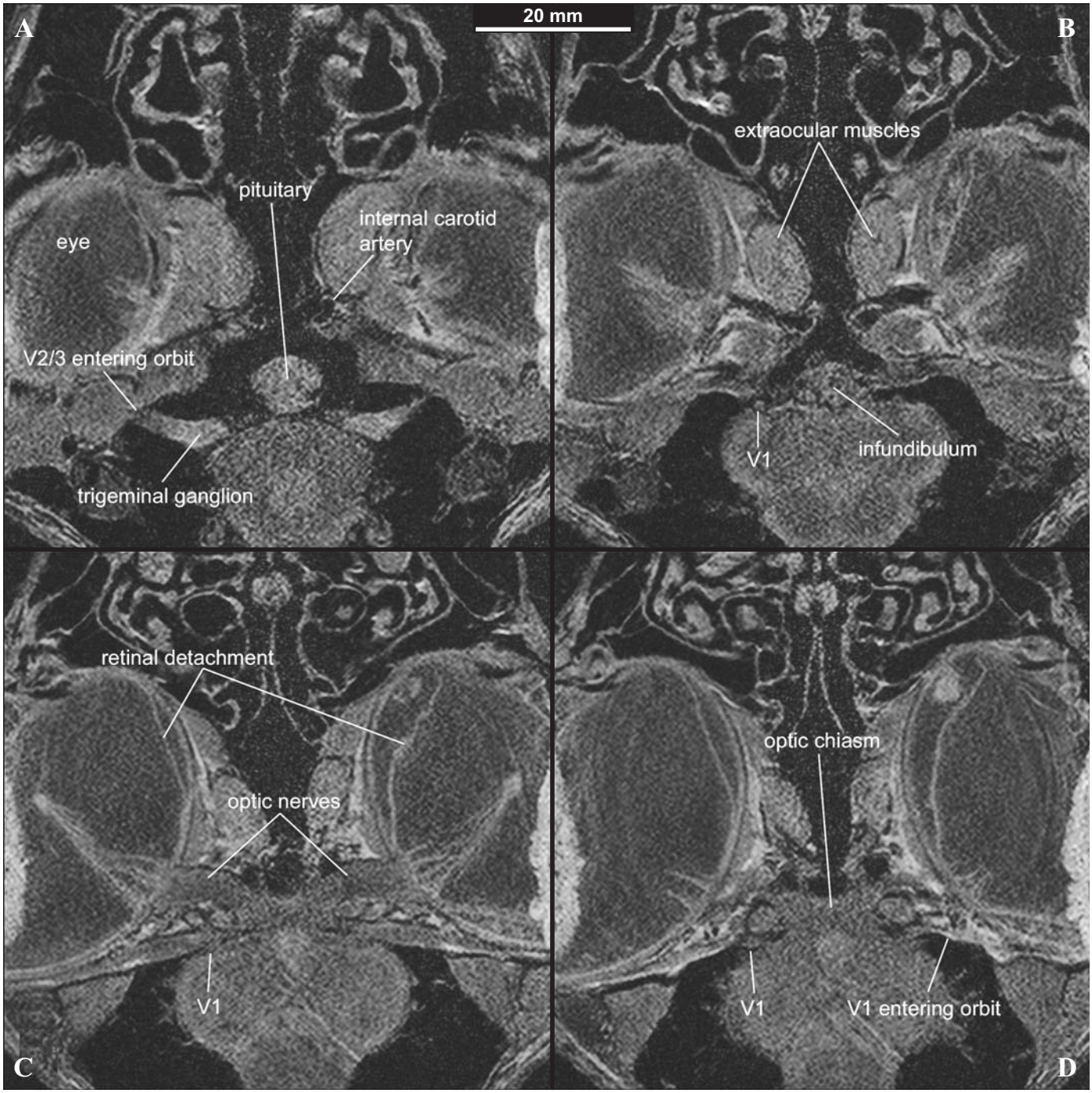

Fig. 8. *Struthio camelus* (LSU-SVM no number, Recent). Axial T1 Gradient echo MRI of showing branches of trigeminal nerve. **A**. Maxillary and mandibular branch trigeminal foramen in posterior orbit. Pneumatized bone of the skull base is black. **B**. V1 ascending the floor of the endocranium. **C**. Optic nerves (II) just distal to the optic chiasm and V1 in the posterior orbital wall. **D**. V1 at the orbital apex on left and entering the orbit on the right. All sections are in the same scale.

additional requirement of neurovascular branches to supply each of their teeth. Most of the upper toothrow of basal theropods, like *Ceratosaurus*, was comprised of the maxilla. Animals with numerous teeth and upper jaws dominated by the maxilla would be expected have larger maxillary nerves/arteries with a relatively smaller contribution from the ophthalmic branch of the trigeminal. In alligators, the maxillary and ophthalmic branches of the trigeminal nerve have adjacent paths towards the superior orbit (Fig. 7). The larger maxillary branch traverses the orbit inferior to the eye and enters the posterior snout and maxillary bone, while the mandibular branch travels ventrally to the hinge of the jaw along the adductor muscles (Schumacher 1973). In *Struthio*, the ophthalmic branch travels from the trigeminal ganglion along the floor of the skull and enters the orbit just posterior and lateral to the optic nerve (Fig. 8). The maxillary division

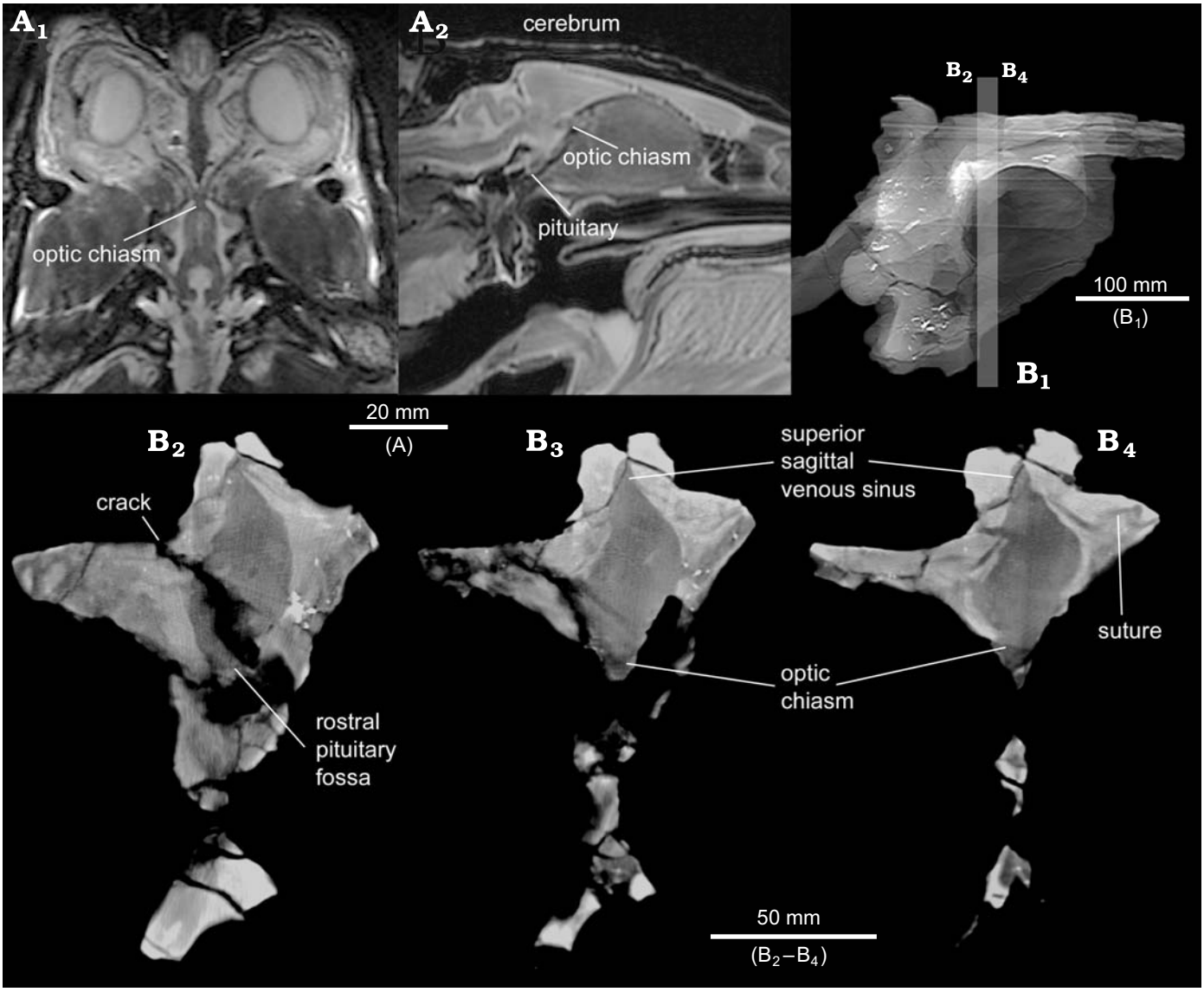

Fig. 9. **A**. *Alligator mississippiensis* (LDWF 904625, Recent), optic/pituitary zone; A_1, axial T2 weighted MRI, showing the optic chiasm in interorbital foramen; A_2, sagittal T2 weighted MR1 of the same specimen, showing the optic chiasm within the interorbital fenestrum. **B**. *Ceratosaurus magnicornis* (MWC 1, Fruita, Colorado, Morrison Formation, Upper Jurassic); B_1, computed tomography image of the whole braincase in right lateral view, with semitransparent slab indicating location of the sections through optic/pituitary zone; B_2–B_4, sections through optic/pituitary zone that progress from caudal to rostral.

branches into several posterior orbital nerves while the mandibular division continues on to the mandibular angle. This same configuration is illustrated in the rooster (Watanabe and Yasuda 1970). In *Ceratosaurus*, the rostral edge of the trigeminal foramen abuts a complex of basisphenoidal sinus cavities in the roof of the pharynx immediately caudal to the pituitary fossa. No recognizable forward projecting foramina/canals were observed, but there is a transversely oriented fracture of the specimen at the caudal margin of the pituitary fossa that complicates interpretation of this region.

Zone 4: Optic/pituitary (Fig. 9).—This region is characterized by the presence of the pituitary fossa. The pituitary fossa is recognized by an abrupt ventral projection of the floor of the endocranium rostral to the trigeminal trunk. The conical pituitary fossa is slightly posteriorly inclined relative to the long axis of the brain. Its contours bear only a gross reflection of the shape of the neural structures it contains: the hypothalamus, tuber cenerum, infundibulum and pituitary gland proper. Surrounding the infundibulum are the optic tracts and their crossing fibers that form the optic chiasm immediately rostral to the infundibulum. The majority of the cerebral hemispheres are situated above the pituitary fossa and there is a marked expansion of the dorsal endocranial cavity in this area. The paired internal carotid arteries and their ophthalmic branches, the ophthalmic veins, and the cranial nerve supplying the orbit (II–VI) all penetrate the braincase through the ventral rostral confines of the endocranium in this zone.

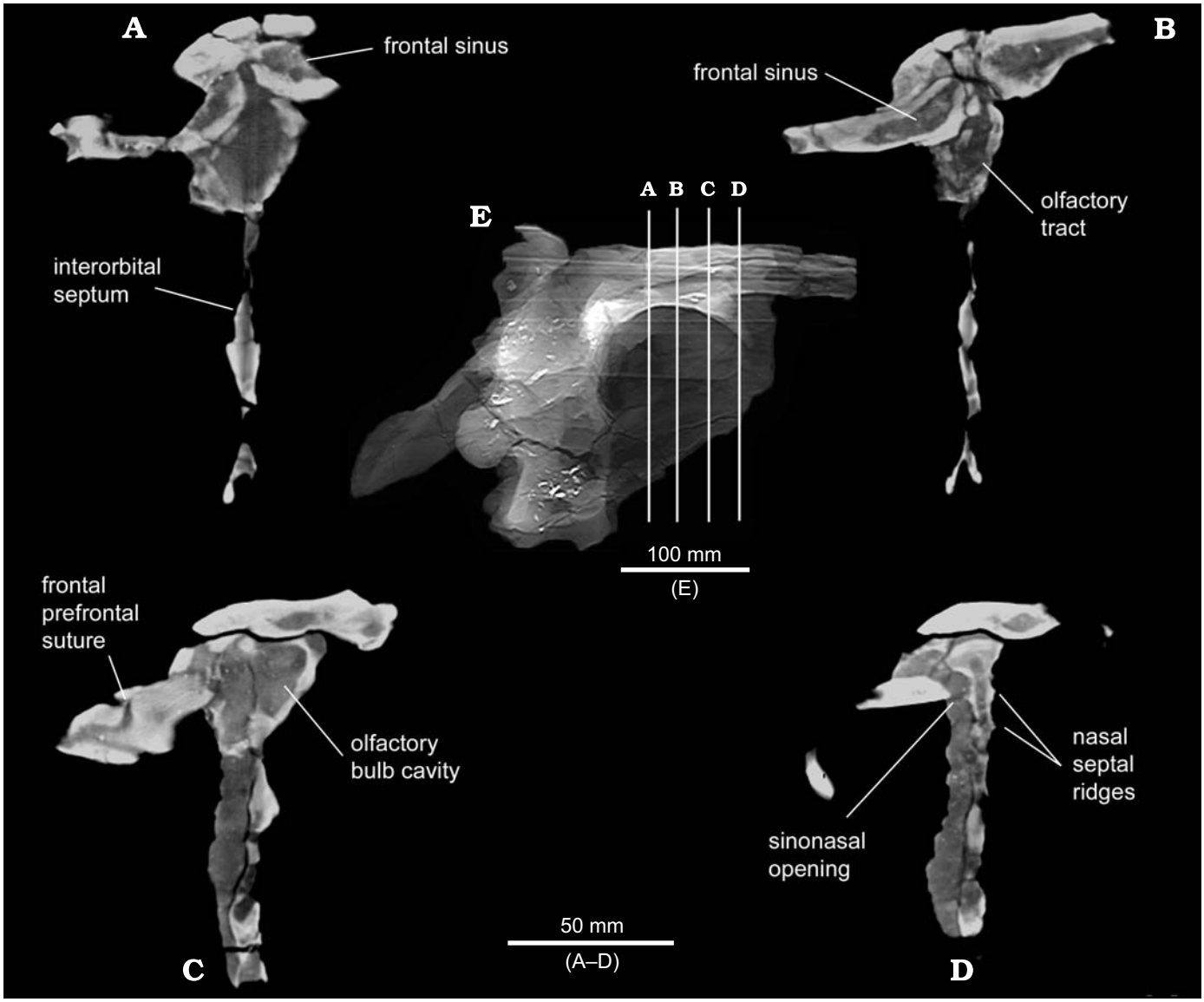

Fig. 10. *Ceratosaurus magnicornis* (MWC 1, Fruita, Colorado, Morrison Formation, Upper Jurassic). **A–D**. Computed tomograms of the olfactory zone. **E**. Right lateral view of the whole braincase with vertical white lines indicating positions of sections A–D.

The previously mentioned fracture at the caudal margin of the pituitary fossa extends to the caudal edge of a prominent interorbital septum (mesethmoid) fenestration positioned at the expected exit of the optic tracts. The fenestration is over a centimeter in diameter with fractured margins. The bone covering of the endocranial endocast at the caudal medial margins of the orbit is extremely thin and no distinct additional foramina were observed. The only large structure to cross between the orbits is the optic chiasm. The position of the optic tract and chiasm dorsally in the orbit is consistent with the eye being situated superiorly in the bony orbit. A similar optic foramen/interorbital septal fenestration is seen in the American alligator (Figs. 7, 9), the interorbital foraminal pattern of many birds and *Tyrannosaurus* (Brochu 2003).

The rostral cerebrum gently tapers into the root of the olfactory tracts. Similar brain and endocranial morphology is shown in alligators where the cerebral hemispheres/olfactory lobes taper into the olfactory tract and the lateral ventricles are continuous with the olfactory ventricles. As there is no discrete morphologic change in the endocranial cavity as it traverses the roof of the orbits, the optic/pituitary zone ends arbitrarily in the rostral margin of the bony orbital rim at the postorbital/prefrontal contact

Zone 5: Olfactory (Fig. 10).—The olfactory zone is dominated by the olfactory tracts. The olfactory tracts travel rostrally in the roof of the snout above a bifurcation of the interorbital septum (ectoethmoid). They share a common sagittal cavity until they reach the rostral border of the orbit where the tracts then expand into the olfactory bulbs. The bulbs are transversely compressed and remain in contact medially. Their ventral surfaces are exposed to the roof of the

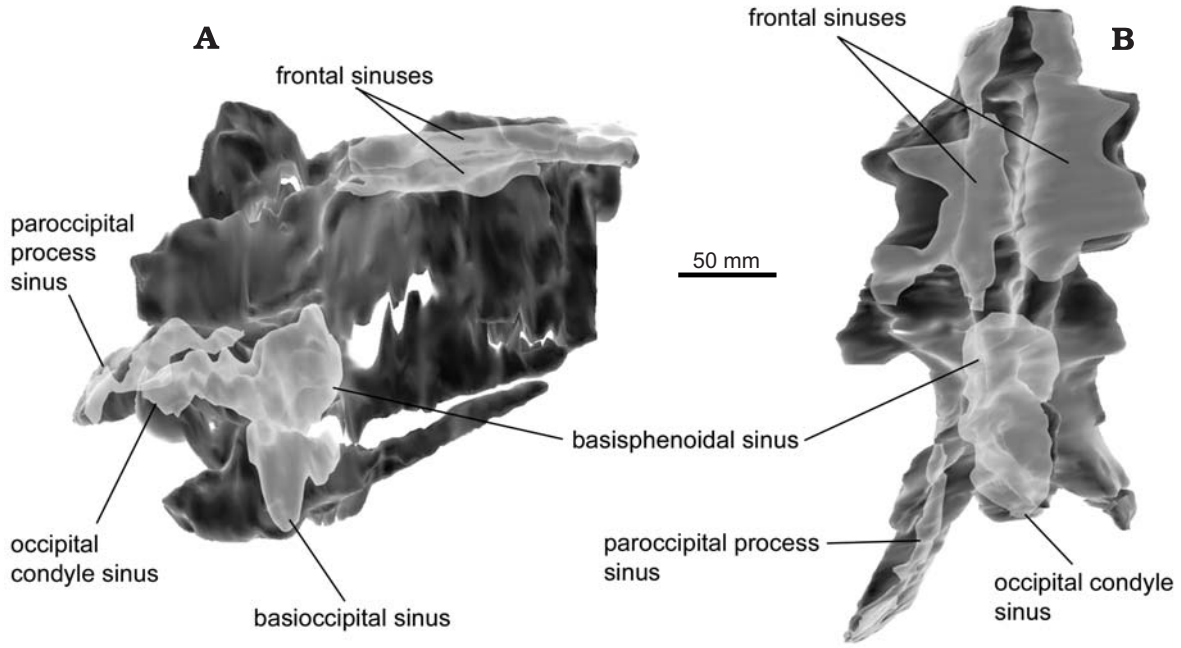

Fig. 11. *Ceratosaurus magnicornis* (MWC 1, Fruita, Colorado, Morrison Formation, Upper Jurassic). Three-dimensional virtual rendering of the preserved pneumatic sinuses in right lateral (**A**) and dorsal (**B**) views.

sinonasal cavity (olfactory region of the cavum nasi proprium) of the snout at about the level of the prefrontal/frontal contact. As with the endocast of *Allosaurus* (UUVP 294), the olfactory bulbs do not occupy the entire portion of the caudal dorsal sinonasal cavity (Rogers 1998). The complete volume of the cavity in *Ceratosaurus* cannot be determined due to the absence of rostral and lateral portions of the skull. The remaining posterior portion of the sinonasal cavity communicates with several dorsal medial openings of the frontal bone forming pneumatic diverticulae (frontal sinuses).

Although the caudal ventral skull base pneumatic cavities are well-preserved, the existence of suborbital or antorbital sinuses (Witmer 1990,1995) cannot be determined.

Cranial pneumatic cavities (Fig. 11).—The basicranial intraosseus pneumatic cavities, or sinuses of *Ceratosaurus*, are camarate in morphology and resemble their cervical vertebral counterparts and so reflect the vertebral origin of the basal skull elements. This pattern probably, in part, resolves the question posed by Witmer (1997b) regarding the tympanic versus pulmonary origin of the subcondylar recesses of ornithomimids, tyrannosaurids, and therizinosaurs in favor of a vertebral/pulmonary origin.

In *Ceratosaurus*, the most caudal intraosseus pneumatic sinus fills the majority of the paroccipital process. The paroccipital process, replete with its quadrate facet, is the skull base equivalent of the vertebral zygapophyseal process and is similarly pneumatized by dorsal intervertebral diverticulae. The paroccipital process sinus cavity communicates with the overlying dorsal soft tissue compartment of the craniocervical junction through several discrete foramina. The larger foramina are close to the base of the paroccipital processes (Fig. 2). Compared to a mature *Allosaurus*, the occipital condyle of *Ceratosaurus* is less pneumatic with small branching camerae being located adjacent the floor of the medullary spinal canal within the proximal and dorsolateral condyle. Camerae, as first proposed by Britt (1993) and later refined by (Wedel 2000), are enclosed pneumatic chambers with rounded and smooth contours, range in size from 5 to 150 mm, and are separated by septa ranging in thickness from 2 to 10 mm. These spaces are contiguous with the branching camerae of the basioccipital sinuses that form flanking camerae at the dorsal apex of the basitubera (tuberous processes). Rostral to the basitubera, there is a second complex of camerae that form the basiphenoidal sinus complex. These camerae are separated from the basioccipital complex by a transverse septum of bone at the basioccipital and basisphenoidal contact in the rostral basitubera (Fig. 4A). The basiphenoidal complex is very similar in morphology to cervical vertebral camerae in that there is a median septum dividing the cavity into roughly symmetrical left and right cavities, as well as having a partial dorsal-ventral division rostrally. The cross-section of the basipterygoid is reminiscent of cervical parapophyses, while the lateral openings of the basiphenoidal sinuses resemble cervical vertebral lateral fossae and central camerae, complete with a rostral first order bifurcation (Fig. 4E). The crista prootica covers the rostral extent of the basiphenoidal camerae (Fig. 6B). The ventral extent of the basiphenoidal complex invades the basipterygoid process. This portion of MWC-1 is partially obscured on the CT images by beam hardening artifact from metallic inclusions. The basiphenoidal sinus complex terminates rostrally at the caudal margin of the orbit. Any antorbital/suborbital pneumatic sinus, as is commonly observed

in birds, shows no apparent osteological correlate in the remaining interorbital septum of MWC 1.

Uncomplicated supraorbital intraosseous pneumatic cavities are found within frontals and remaining portion of the right prefrontal process (Fig. 10). Caudally, they meet at the midline superficial to the superior sagittal venous sinus at the junction of the cerebrum and olfactory tracts. The right frontal sinus maintains a long communication with the cavity of the olfactory tract, while the left remains separate. There are no direct superficial or orbital communications from the frontal sinuses. Both appear to extend into the contacts with the missing lacrimal bones, however. In birds, the lacrimal is pneumatized by a diverticulm of the antorbital sinus and the prefrontal is lost/absent (Witmer 1995). Osteological cranial facial pneumatic features in therapods has in general not received much descriptive attention in the literature largely because there are few intact skulls and even fewer that have been scanned. Reevaluation of disarticulated skull material by CT scanning is very likely to yield previously undetected pneumatic anatomy. We recently scanned an as of yet uncataloged *Alioramus* skull that also demonstrated frontal sinus pneumatization in this primative tyrannosaur.

The olfactory tracts terminate in distinct expansions of the ectoethmoids near the prefrontal contact with the nasals. There is a partial median septation that defines the left and right olfactory bulbs. Rostrally, the left and right bulb cavities are further partially divided into dorsal and ventral divisions. The rostral ends of the olfactory bulb cavities communicate widely with the roof of the posterior sinonasal cavity of the snout. How much of this space was occupied by the nasolacrimal ducts is unknown. Close inspection of the remaining sinonasal septum, rostral to the termination of the olfactory bulbs, reveals paired ridges (Fig. 10D) in the dorsal region of the septum. As this region is normally associated with the olfactory apparatus, and caudal conchal structures are known in birds (Bang and Wenzel 1985; Fitzgerald 1969), it is easy to speculate that these ridges may have been associated with caudal conchal structures. The caudal concha of *Struthio camelus* (Fig. 12) are quite small and do not appose a midline sinonasal septum. Rather, they are widely separated by the very inflated pneumatized mesoethmoid and vomer. More rostrally, however, there are ridges along the ventral caudal vomerine portion of the nasal septum that illustrate how this midline structure reflects the presence of the caudal portion of the middle concha that arise from the lateral wall of the sinonasal cavity.

Cranial venous sinuses (Fig. 13).—A three-dimensional representation of the above venous structures of *Ceratosaurus* reveals that the cerebral venous sinuses constitute the confluence of both the deep cerebral and superficial meningeal draining veins that carry blood away from the brain and into the internal jugular veins and the perimedullary/spinous venous sinus (Zippel et al. 2003; Hopson 1979). Two major structures have been previously identified in allosaur endocasts: the middle cerebral vein and the midline longitudinal sinus (Hopson 1979; Rogers 1998). The middle cerebral vein overlies the optic tectum and drains dorsolaterally and caudally. In the allosaur endocast, this vein terminates in a broken endocast of a "probable venous channel"(Hopson 1979) that protrudes from the surface of the endocranium. In MWC-1, the left venous channel extension of the middle cerebral vein is significantly larger than the right and is completely encased in bone throughout its course caudal and superficial to the otic portion of the endocranium (Fig. 4C). Rostral to the otic zone, the middle cerebral vein ascends the skull, traveling dorsally and medially to fuse with the opposite middle cerebral vein to become the superior sagittal venous sinus (longitudinal sinus) at the vertex of the endocranium. This triple confluence is the torcula (Fig. 4C). From here, the superior sagittal venous sinus follows the dorsal midline of the endocranium to at least the base of the olfactory tracts. In the caimans, this sagittal sinus has been shown to extend to the olfactory bulb plexus (Hopson 1979). In cross-sectional images of the endocranium, the superior sagittal venous sinus would occupy the apex of the triangular roof of the endocranium (Figs. 6A, 8A, 9E). Additional intracranial venous structures were undoubtedly present, but as they did not occupy a position against the inner surface of the endocranial cavity, they can only be inferred based on comparative anatomical grounds (Hopson1979).

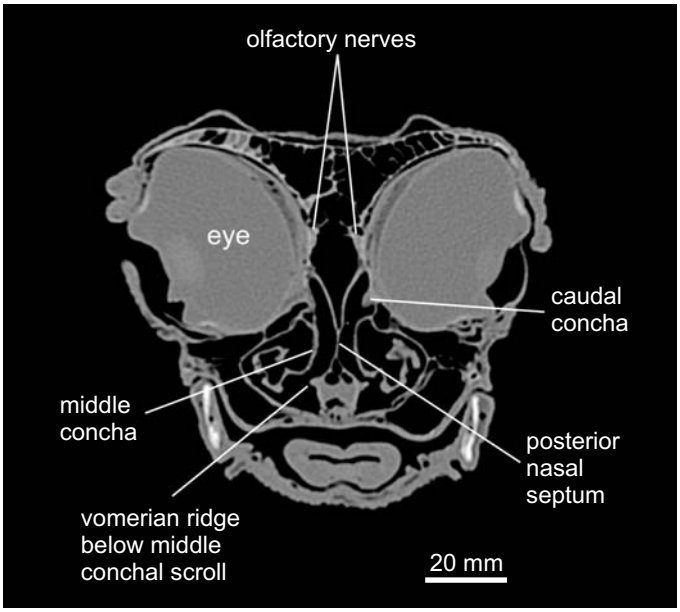

Fig. 12. *Struthio camelus* (LSU-SVM no number, Recent). Coronal oblique CT image of the head, showing the relationship of the caudal nasal septal ridge along the ventral vomer to the adjacent caudal portion of the middle concha. The concavity of the septum mirrors the curve of the concha.

Discussion

Through the application of computed tomography, several potentially important morphological features of ceratosaurian endocranial anatomy have been demonstrated and

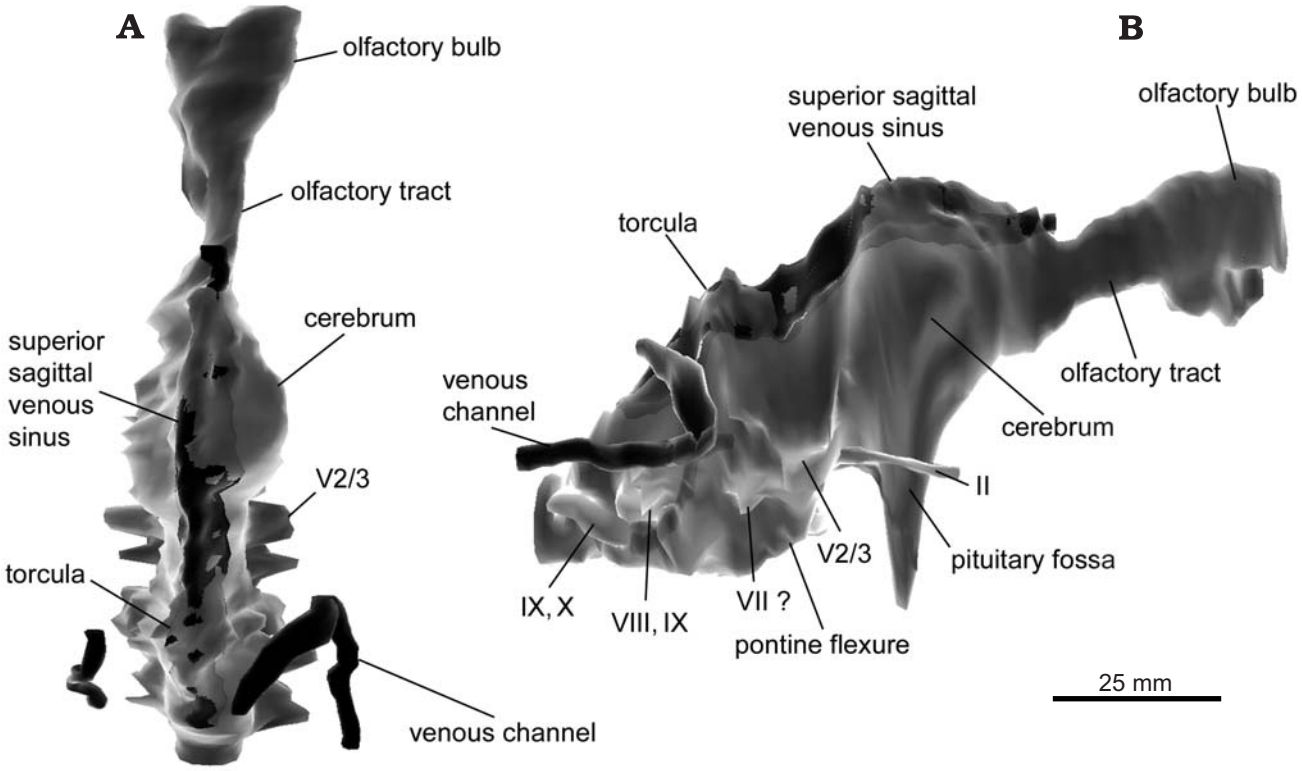

Fig. 13. *Ceratosaurus magnicornis* (MWC 1, Fruita, Colorado, Morrison Formation, Upper Jurassic). Three-dimensional digital reconstruction of the endocraniuim and associated venous structures in dorsal (**A**) and right lateral (**B**) views. Venous structures are shown in black.

are summarized in the three-dimensional reconstruction of Fig. 14. We divided the endocranium into discrete anatomic zones to assist in future CT comparisons. Each zone is readily identifiable by the aforementioned dominant morphologic features. Hopefully, this breakdown will also serve to facilitate discussion of the functional segmentation of the endocranium and its relevance to functional morphology/paleoneurobiology. As the pool of comparative data is still very small and generally not publicly available, strong conclusions regarding evolutionary trends and the functional/behavioral significance of certain anatomical features can only be tentative at best. With this caveat in mind, we offer the following observations.

The obtuse occipitofrontal angle of the basicranium and relatively unflexed shape of the endocranium seem to support a horizontal craniocervical posture. This inference is further supported by the slightly upturned position of the snout when the horizontal semicircular canal is parallel the ground surface. How these anatomic relationships change in more derived theropods has yet to be determined.

The similarity of the semicircular canal configuration of *Ceratosaurus* to other basal tetanuran theropods has been confirmed. This conserved configuration is likely a product of similar biomechanical constraints for terrestrial locomotion. Relative enlargement of the anterior semicircular canal has recently been shown to correspond with habitual bipedal rather than quadrupedal locomotion (Sipla et al. 2004). The size and shape of the cochlear duct may also prove to be another interesting aspect of the otic anatomy. As has been shown in crocodilians (Wever 1978) and birds (Smith 1985) the frequency discrimination of the ear can be roughly correlated with the relative length of the basilar membrane and therefore the cochlear duct. A direct comparison of cochlear duct shapes and sizes among dinosaurs in general, let alone among theropods specifically, has yet to be made. However, this correlation raises an interesting avenue for functional morphologic evaluation among dinosaur groups suspected of being social by virtue of nesting behavior, sexual dimorphism, and particularly in having nasal crests capable of producing vocalization. More elaborate and elongate cochlear ducts typically include the addition of higher frequencies. Short cochlear ducts reflect hearing restricted to lower frequencies. Short cochlear ducts do not preclude infrasound vocalization between adults, but hatchling animals are generally not attributed with the ability to produce infrasound and vocalize at higher frequencies.

Comparison of basicranial foraminal patterns in theropods is quite difficult owing to the variety of foraminal patterns. Computed tomography is useful in facilitating the correct identification of foramina by demonstrating the endocranial origin of the nerve or vascular structure in question. It is also helpful in identifying foramina that are not apparent from the surface of the specimen either because of inadequate preparation or poor preservation. By comparing foraminal patterns in birds with narrow *versus* wide skull mor-

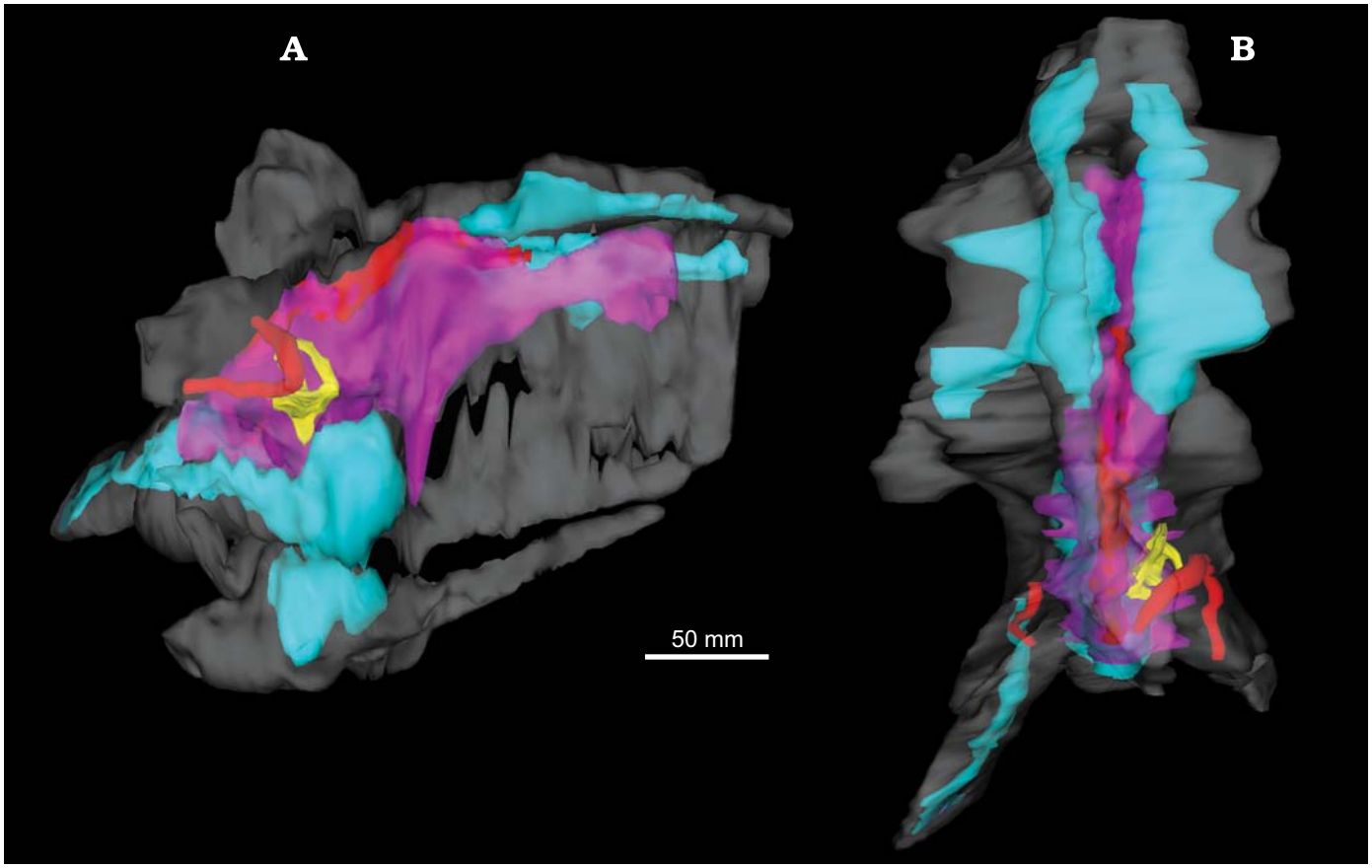

Fig. 14. *Ceratosaurus magnicornis* (MWC 1, Fruita, Colorado, Morrison Formation, Upper Jurassic). Summary three-dimensional digital reconstruction featuring the skull overlay in grey, endocranium in violet, inner ear in yellow, pneumatic sinuses in light blue, and venous sinuses in red, in right lateral (**A**) and dorsal (**B**) views.

phologies, we have observed a general increase in the number and spatial separation of foraminal openings with an increase in distance of the skull surface from the endocranium proper. In *Ceratosaurus*, the narrow configuration of the skull more tightly apposes the cranium to the surface of the brain and there is a subsequent decrease in foraminal openings. Small cranial nerves, particularly III, IV, and VI, may have shared foramina or fissures near II and V1. Based on our observations of V1 in alligator and bird skulls, the relative sizes of the foramina of V1 and V2 can vary considerably, thus further confusing the foraminal interpretation of a specimen based on external inspection alone. Nonavian therapod skulls with large tooth-bearing maxilla are likely to have a large V2 branch that resembles the condition demonstrated in alligators. The premaxilla dominated skulls of edentulous birds have a reduced periorbital distribution of V2 and are therefore considered an inappropriate model for trigeminal nerve anatomy reconstruction and forminal identification in basal tenurians. Additionally, a single optic foramen, especially when associated with an opening in the interorbital septum, reflects the location of the optic chiasm as the optic nerves proper are frequently located outside the cranium in an interorbital location in extant birds and alligators that display this foraminal pattern.

The pneumatization of the occipital condyle of *Ceratosaurus* is less elaborate than that shown in *Allosaurus*. In all other respects, the skull pneumatization is quite extensive. Pneumatic sinuses are found within the paroccipital processes and basiocciput of *Ceratosaurus*. The camerate morphology of basicranial skull pneumatization mirrors similar pneumatic morphology of the cervical spine, which shares a common developmental origin and relationship to the cervical vertebral pneumatic diverticula. The basiphenoid complex was introduced and assigned a separate pneumatic sinus designation from the previously described median epipharyngeal recess. We also described pneumatization of the frontal bone complex and discussed the probability of its relationship to extraosseous orbital pneumatization as seen in birds. The olfactory apparatus of MWC-1 is well preserved and yields what appears to be an accurate depiction of the olfactory bulb anatomy. They are not as greatly exaggerated as in *Tyrannosaurus* (Brochu 2000, 2003). As *Ceratosaurus* was a moderate sized theropod relative to the latter taxon, this observation supports the hypothesis that the olfactory lobes of *Tyrannosaurus* were developed beyond what would be expected by simple allometry (Holtz 2004). The roof of the posterior sinonasal cavity is intact and parallel ridges along the posterior dorsal nasal septum raise the possibility of olfactory conchae having been

present in MWC 1. Particular attention to this region of the skull in future comparisons is likely to yield previously overlooked/unsuspected evidence of elaborate olfactory apparatuses. Intact skulls should, therefore, be scanned prior to preparation in this region to avoid losing subtle indications of conchal anatomy within matrix.

Dural-based endocranial venous sinuses often leave traces within the inner surfaces of the basicranium and can be identified with CT scanning and endocranial reconstruction. Patulous venous structures more intimately apposed to the brain's surface are less reliably identified. In MWC 1, we were able to identify the superior sagittal venous sinus (longitudinal sinus), torcula, and middle cerebral vein. Asymmetry in the caliber between the left and right systems was demonstrated. As the cerebrospinal fluid and endocranial venous structures comprise a significant volume of the endocast, estimations of brain volume based on endocasts should include some correction or account of this space. The gross morphology of theropod brains is similar to crocodilian brains and exhibit a similar olfactory, cerebral, tectal, and cerebellar/medullary morphology.

Acknowledgments

We wish to thank John Foster (MWC) for permission to CT scan the specimen of *Ceratosaurus* and Ray Wilhite (LSU-SVM) for access to his comparative anatomy resources including alligator and ostrich specimens. We also thank Peter M. Galton (University of Bridgeport, College of Naturopathic Medicine, Bridgeporte, CT) and Ralph E. Molnar (Museum of Northern Arizona, Flagstaff) for their constructive comments on the preparation of this manuscript.

References

Bang, B. and Wenzel, B. 1985. Nasal cavity and olfactory system. *In*: A. King and J. McLelland (eds.), *Form and Function in Birds*, 195–225. Academic Press. London.

Britt, B.B. 1993. *Pneumatic Postcranial Bones in Dinosaurs and Other Archosaurs*. 383 pp. Unpublished Ph. D. thesis. University of Calgary, Calgary.

Brochu, C.A. 2000. A digitally-rendered endocast for *Tyrannosaurus rex*. *Journal of Vertebrate Paleontology* 20: 1–6.

Brochu, C.A. 2003. Osteology of *Tyrannosaurus rex*: Insight from a nearly complete skeleton and high-resolution computed tomographic analysis of the skull. *Society of Vertebrate Paleontology Memoir* 7: 1–138.

Burda, D.J. 1969. Developmental aspects of intracranial arterial supply in the alligator brain. *Journal of Comparative Neurology* 135: 369–380

Coria, R.A. and Currie, P.J. 2003. The braincase of *Giganotosaurus carolinii* (Dinosauria: Theropoda) from the Upper Cretaceous of Argentina. *Journal of Vertebrate Paleontology* 22: 802–811.

Chiasson, R. 1962. *Laboratory Anatomy of the Alligator*. 56 pp. W.M.C. Brown Company Publishers, Dubuque, Iowa

De Beer, G.R. 1947. How animals hold their heads. *Proceedings of the Linnean Society of London* 159: 175–139.

Dujim, M. 1951. On the head posture in birds and its relation to some anatomical features. *Proceedings of the Koninklijke Nederlandse Akademie Van Wetenschappen, Series C. Biological and Medical Sciences* 54: 260–271.

Erichsen, J.T., Hodos, W., Evinger, C., Bessette, B.B., and Phillips, S.J. 1989. Head orientation in pigeons: postural, locomotor and visual determinants. *Brain Behavior Evolution* 33: 268–27.

Fitzgerald, T. 1969. Splanchnology. *In*: *The Coturnix Quail Anatomy and Histology*, 239–243. Iowa State University Press, Ames, Iowa.

Gilmore, C.W. 1920. Osteology of the carnivorous Dinosauria in the United States National Museum, with special reference to *Antrodemus* (*Allosaurus*) and *Ceratosaurus*. *Bulletin of the United States National Museum* 110: 1–154.

Holtz, T.R. 2004. Tyrannosauroidea. *In*: D.B. Weishampel, P. Dodson, and H. Osmólska (eds.), *The Dinosauria* (second edition), 111–136. University of California Press, Berkeley, California.

Hopson, J.A. 1979. Paleoneurology. *In*: C. Gans, R.G. Northcutt, and P. Ulinski (eds.), *Biology of the Reptilia, Vol. 9*, 39–146. Academic Press, New York.

Kuhne, R. and Lewis, B.1985. External and middle Ears. *In*: A. King and J. McLelland (eds.), *Form and Function in Birds, Vol. 3*, 227–271. Academic Press, London.

Larsson, H. 2001. Endocranial anatomy of *Carcharodontosaurus saharicus* (Theropoda: Allosauroidea) and its implications for theropod brain evolution. *In*: D. Tanke and K. Carpenter (eds.), *Mesozoic Vertebrate Life*, 19–33. Indiana University Press, Indianapolis.

Madsen, J. and Welles, S. 2000. *Ceratosaurus* (Dinosauria, Theropoda): A revised osteology. *Utah Geological Survey Miscellaneous Publication* 2: 1–80.

Marsh, O. 1896. The dinosaurs of North America. *Annual Report of the United States Geological Survey* 16: 133–244.

Rogers, S.W. 1998. Exploring dinosaur neuropaleobiology: viewpoint computed tomography scanning and analysis of an *Allosaurus fragilis* endocast. *Neuron* 21: 673–679.

Rogers, S.W. 1999. *Allosaurus*, crocodiles, and birds: evolutionary clues from spiral computed tomography of an endocast. *The Anatomical Record* 257: 162–173.

Schumacher, G. 1973. The Head muscles and hyolaryngeal skeleton. *In*: C. Gans and T. Parsons (eds.), *Biology of the Reptilia*, 109–199. Academic Press. London.

Sipla, J., Georgi, J., and Forster, C. 2004. The semicircular canals of dinosaurs: tracking major transitions in locomotion. *Journal of Vertebrate Paleontology* 24: 113A.

Smith, C.A. 1985. Inner ear. *In*: A.S. King and J. McLellan (eds.), *Form and Function in Birds*, 273–310. Academic Press, London.

Watanabe, T. and Yasuda, M. 1970. Comparative and topographical anatomy of the fowl XXVI: Peripheral course of the trigeminal nerve. *The Japanese Journal of Veterinary Science* 32: 43–57.

Wedel, M.J., Cifelli, R.L., and Sanders, R.K. 2000. Osteology, paleobiology, and relationships of the sauropod dinosaur *Sauroposeidon*. *Acta Palaeontologica Polonica* 45: 343–388.

Wever, E.G. 1978. Chapter 24. Order Crocodilia: The crocodiles. *In*: *The Reptile Ear: Its Structure and Function*, 924–964. Princeton University Press, Princeton, New Jersey.

Witmer, L.M. 1995. Homology of facial structures in extant archosaurs (birds and crocodilians), with special reference to paranasal pneumaticity and nasal conchae. *Journal of Morphology* 225: 269–327.

Witmer, L.M. 1997a. The evolution of the antorbital cavity of archosaurs: A study in soft-tissue reconstruction in the fossil record with an analysis of the function of pneumaticity. *Journal of Vertebrate Paleontology* 17, *Memoir* 3: 1–73.

Witmer, L.M. 1997b. Craniofacial air sinus systems. *In*: P.J. Currie and K. Padian (eds.), *Encyclopedia of Dinosaurs*, 151–159. Academic Press, New York.

Zippel, K.C., Lillywhite, H.B., and Mladinich, C.R.J. 2003. Anatomy of the crocodilian spinal vein. *Journal of Morphology*. 258: 327–335.